

## The usefulness of $^{18}\text{F}$ -FDG PET images obtained 2 hours after intravenous injection in liver tumor

Koichi KOYAMA,\* Terue OKAMURA,\* Joji KAWABE,\*\* Nozomi OZAWA,\*  
Shigeaki HIGASHIYAMA,\* Hironobu OCHI\*\* and Ryusaku YAMADA\*

*Departments of \*Radiology and \*\*Nuclear Medicine, Osaka City University School of Medicine*

Liver tumors, especially hepatocellular carcinomas (HCCs), often exhibit no contrast with surrounding non-tumorous liver tissue in F-18-fluoro-2-deoxy-2-fluoro-D-glucose (FDG) positron emission tomography (PET) images obtained at the usual interval of one hour after intravenous FDG injection. We evaluated the usefulness of FDG PET studies of liver tumors performed 2 hours after intravenous injection. **Methods and Materials:** Fifteen pretherapeutic patients with 33 liver tumors were studied, including 11 patients with 18 HCCs, and 4 patients with 15 metastatic liver tumors (METAs) from 3 colorectal carcinomas and 1 esophageal carcinoma. After transmission scans, emission scans were obtained 45–55 minutes and 115–125 minutes after intravenous injection of 185–370 MBq FDG as early images and delayed FDG PET images, respectively. Visual analysis of early and delayed images was performed, and the FDG uptake in the tumor to that in non-tumorous liver ratio (T/N ratio), the FDG uptake in tumor to that in soft-tissue ratio (T/S ratio) and the FDG uptake in non-tumorous liver to that in soft-tissue ratio (N/S ratio) were calculated for each image. **Results:** In visual analysis, visual improvement seen in images was observed in 6 of 18 HCC lesions and all 15 META lesions. In quantitative analysis, the mean T/S ratio and T/N ratio of HCCs in early images were 4.97 and 1.90, respectively, and those in delayed images were 6.24 and 2.20, respectively. The mean T/S ratio and T/N ratio of METAs in early images were 5.97 and 2.21, respectively, and those in delayed images were 6.99 and 3.80, respectively. The T/S ratio of HCCs and T/S ratio and T/N ratio of METAs were significantly higher in delayed images than in early images. The mean N/S ratios of HCC cases were 2.58 in the early images and 2.57 in the delayed images, but the ratio showed no constant tendency in the images. All N/S ratios of META cases were decreased in delayed images, although the significance of the difference between early and delayed images in N/S ratios was not analyzed because of the small number of cases. **Conclusion:** FDG PET studies performed 2 hours after intravenous injection were useful for clear visualization of liver tumors, especially metastatic liver tumors.

**Key words:** liver, FDG PET, hepatocellular carcinoma, metastatic liver tumor

### INTRODUCTION

IN NUCLEAR MEDICINE IMAGING, positron emission tomography (PET) with F-18-fluoro-2-deoxy-D-glucose (FDG) is

now established as a method for clinical diagnosis to reveal malignancies by evaluating the glucose metabolism of the tissue. The clinical usefulness has been reported in various tumors such as brain, lung and pancreas.<sup>1–5</sup>

Received March 14, 2001, revision accepted January 10, 2002.

For reprint contact: Koichi Koyama, M.D., Department of Radiology, Osaka City University, 1–5–7, Asahi-machi, Abeno-ku, Osaka 545–8585, JAPAN.

E-mail: koichikoyama@mac.com

For the diagnosis of liver tumors such as hepatocellular carcinomas (HCCs) and metastatic liver tumors (METAs), many investigators have reported the evaluation of FDG PET.<sup>6–10</sup> FDG uptake by tumors in the liver is sometimes unclear, because a high FDG accumulation is not always found in liver tumors, especially in HCCs. FDG PET

images are usually obtained at 1 hour after intravenous FDG injection, but malignant tumors have a high glucose metabolism and continue to gradually accumulate FDG.<sup>11</sup> We therefore speculated that it might be possible to obtain clear images if FDG PET imaging was performed after the usual one hour interval.

The purpose of this study was to evaluate the usefulness of FDG PET images in liver tumors obtained at 2 hours after injection compared with images obtained at about 1 hour after intravenous injection.

## MATERIALS AND METHODS

### *Patients*

Fifteen pretherapeutical patients (10 men and 5 women, age 61 to 83 y.o., mean 66.5 y.o.) with 33 liver tumors underwent FDG PET in our hospital from June 1998 to February 2001 after written informed consent was obtained. All patients underwent computed tomography (CT) imaging with a helical CT imaging system. Eleven patients had 18 HCC lesions and all patients had liver cirrhosis (LC), and the grades of LC were evaluated by means of the Child-Pugh (C-P) score and the clinical stage. Four patients had 15 META lesions from 3 colorectal carcinomas and 1 esophageal carcinoma and none of these 4 patients had LC. Tumor sizes were measured by CT imaging.

Prior to FDG PET studies, blood sugar (BS) levels of all the patients were measured (normal range: 70–105 mg/dl).

### **FDG PET**

#### *FDG PET imaging*

FDG was produced with the NKK-Oxford superconducting cyclotron and NKK synthesis system. A HEADTOME IV SET-1400W-10 (Shimadzu Corp., Kyoto, Japan), which has 4 detector rings providing 7 contiguous slices at 13 mm intervals, was employed for the PET studies. The effective spatial resolution was 14 mm in FWHM.

Before emission scanning, transmission scans were performed for 10 minutes with a <sup>68</sup>Ge/<sup>68</sup>Ga ring source for attenuation correction. Images were obtained from 45 to 55 minutes (early image) and 115 to 125 minutes (delayed image) after intravenous injection of 185–370 MBq FDG. Patients fasted from at least four hours before the beginning of examination to the end of examination.

#### *FDG PET analysis*

##### *Visual analysis:*

The early and delayed FDG PET images were estimated by visual interpretation referring to CT imaging, and regions of FDG accumulation that were stronger than the background uptake were considered to be abnormal. Visual improvement by delayed image compared with early image was also analyzed, and this means that the delayed image showed more intense accumulation in the lesion than the early image.

##### *Quantitative analysis:*

With reference to CT imaging, the region of interest (ROI: circle 6 mm in diameter) was placed in the highest FDG accumulation area in the suspected tumor and other ROIs (circles 20 mm in diameter) were placed in the non-tumorous liver tissue and in the soft tissue behind the lumbar spine as the background. The mean count per voxel of ROIs was used. The ratio of FDG uptake in the tumor to that in soft-tissue (T/S ratio), the FDG uptake in non-tumorous liver to that in soft-tissue ratio (N/S ratio) and the FDG uptake in tumor to that in non-tumorous liver ratio (T/N ratio) of HCCs and METAs were determined and investigated.

The Wilcoxon signed-ranks test was used to analyze data. A p value of less than 0.05 was considered significant.

## RESULTS

The details of all patients, BS, clinical stage, C-P score, tumor size, T/S ratio and T/N ratio of all hepatic lesions, N/S ratio of all cases and visual improvement in delayed image are shown in Table 1. Seven patients showed had a BS level above the normal range, but their BS levels did not exceed 130 mg/dl. All HCC patients had LC, and most of which were in clinical stage as 1 and the C-P score was score A.

#### *Visual analysis*

Visual analysis data are shown in Table 2. Of eighteen HCC lesions, 9 in early images and 10 in delayed images were visually diagnosed. Visual improvement in delayed images was observed in 5 of 9 lesions compared with early images. FDG accumulation was detected in delayed images in 1 lesion, in which FDG accumulation was not detected in early images, but no visual improvement was observed in the remaining 12 lesions. All 15 META lesions could be diagnosed by means of early images, and visual improvement was observed in all of them in delayed images.

#### *Quantitative analysis*

##### *T/S ratio:*

In early images of HCCs, T/S ratios ranged from 1.28 to 9.89 (mean  $\pm$  SD = 4.97  $\pm$  2.44), whereas those in delayed images ranged from 1.12 to 12.93 (mean  $\pm$  SD = 6.24  $\pm$  3.72). In delayed images, T/S ratios increased in 13 of 18 HCC lesions, and there were significant differences between early and delayed images in T/S ratios ( $p = 0.0096$ ) (Fig. 1).

In early images of META lesions, T/S ratios ranged from 4.69 to 7.49 (mean  $\pm$  SD = 5.97  $\pm$  1.01), whereas those in delayed images ranged from 5.07 to 10.43 (mean  $\pm$  SD = 6.99  $\pm$  1.51). In delayed images, T/S ratios increased in 14 of 15 META lesions, and there were significant differences between early and delayed images in T/S ratios ( $p = 0.0054$ ) (Fig. 1).

**Table 1** Details of the data in all hepatic lesions

Pt. No.	sex	age	disease	BS level (mg/dl)	hepatitis virus	liver cirrhosis		location		tumor size (mm)	T/S ratio		T/N ratio		N/S ratio		visual judgment		
						clinical stage	C-P score	upper row: n = 18	lower row: n = 15)		early	delayed	early	delayed	early	delayed	early	delayed	early
1	M	72	HCC	115	C	+	1	A	S6	32 × 47 × 50	3.70	4.03	1.69	1.21	2.18	3.32	-	-	not improved
2	M	65	HCC	105	C	+	1	A	S1	40 × 20 × 35	5.92	5.11	1.61	2.19	3.68	2.33	+	+	not improved
3	M	63	HCC	90	C	+	1	A	S3	40 × 33 × 45	4.20	5.38	1.14	2.31			-	+	improved
4	M	61	HCC	96	C	+	1	A	right lobe portal thrombus	45 × 45 × 50 25 × 75 × 40	5.42 4.69	6.31 7.42	2.12 1.83	2.20 2.59	2.55	2.86	+	+	not improved
5	F	73	HCC	127	C	+	1	A	S3	15 × 15 × 15	6.76	10.63	2.23	2.56	3.04	4.14	+	+	improved
6	M	65	HCC	108	C	+	1	A	S3	10 × 15 × 10	6.23	7.02	2.05	1.70			+	+	not improved
7	F	63	HCC	66	C	+	2	B	S3	10 × 10 × 10	9.06	12.18	2.99	2.94			+	+	improved
8	M	70	HCC	118	no	+	1	A	S8	10 × 10 × 10	3.84	5.67	1.27	1.37			-	-	not improved
9	M	67	HCC	109	C	+	1	A	portal thrombus	50 × 65 × 35	9.89	12.50	3.26	3.02			+	+	not improved
10	F	54	HCC	89	C	+	1	A	S2	15 × 15 × 20	2.90	2.24	1.55	1.45	1.87	1.54	-	-	not improved
11	F	60	HCC	79	C	+	1	B	S5/8	12 × 10 × 20	3.50	4.31	1.01	1.29	3.47	3.34	-	-	not improved
12	F	83	META*	106	no	-	1	A	S8	20 × 30 × 20	2.17	2.10	1.18	1.16	1.84	1.81	-	-	not improved
13	M	61	META**	108	no	-	1	A	S2	50 × 45 × 40	1.90	2.34	1.03	1.30			-	-	not improved
14	M	63	META*	96	no	-	1	B	S5	15 × 13 × 20	1.28	1.12	1.54	1.58	0.83	0.71	+	+	improved
15	M	78	META*	81	no	-	1	A	S5	20 × 16 × 20	4.71	3.54	1.25	1.16	3.76	3.04	+	+	not improved
									S7	15 × 15 × 15	4.77	7.58	2.41	3.42	1.98	2.22	+	+	improved
									S5/8	40 × 30 × 63	8.60	12.93	4.00	6.11	2.15	2.12	+	+	improved
									S8	30 × 42 × 30	4.77	5.55	1.81	2.37	2.63	2.34	+	+	improved
									S3	21 × 26 × 20	6.81	9.39	2.74	4.40	2.48	2.13	+	+	improved
									S4/8	15 × 18 × 20	5.33	8.22	2.15	3.85			+	+	improved
									S4	31 × 31 × 60	7.25	10.43	2.92	4.89			+	+	improved
									S4-S3	120 × 70 × 100	5.65	6.34	2.65	4.05	2.13	1.57	+	+	improved
									S5	35 × 35 × 50	5.29	5.84	2.48	3.73			+	+	improved
									S6	15 × 15 × 20	4.82	5.21	2.26	3.33			+	+	improved
									S1	15 × 10 × 10	5.31	5.07	2.49	3.24			+	+	improved
									S4/8	30 × 30 × 30	7.49	7.80	2.31	4.33	3.24	1.80	+	+	improved
									S8	30 × 40 × 30	7.19	7.43	2.22	4.12			+	+	improved
									S5	40 × 30 × 40	6.93	6.98	2.14	3.87			+	+	improved
									S5/7	25 × 20 × 20	5.36	6.52	1.65	3.62			+	+	improved
									S6	30 × 30 × 35	5.73	7.15	1.77	3.96			+	+	improved
									S3	40 × 20 × 40	4.69	6.98	1.45	3.87			+	+	improved
									S3	20 × 30 × 20	6.96	5.97	2.15	3.31			+	+	improved

M; male, F; female, HCC; hepatocellular carcinoma, META\*; metastatic liver tumor from colon cancer, META\*\*; metastatic liver tumor from esophageal cancer, BS level; blood sugar level, C; hepatitis virus type C, no; no hepatitis virus, C-P score; Child-Pugh score, T/S ratio; tumor to soft-tissue ratio, T/N ratio; tumor to non-tumorous liver ratio, N/S ratio; non-tumorous liver to soft-tissue ratio, early; early image of FDG PET, delayed; delayed image of FDG PET, +; visually detected, -; not visually detected

**Table 2** Summarized visual analysis of all hepatic lesions

early image	delayed image	Visual improvement	HCC	META
-	-	not improved	8	0
-	+	improved	1	0
+	+	not improved	4	0
+	+	improved	5	15
total			18	15

HCC; hepatocellular carcinoma, META; metastatic liver tumor, +; visually detected, -; not visually detected

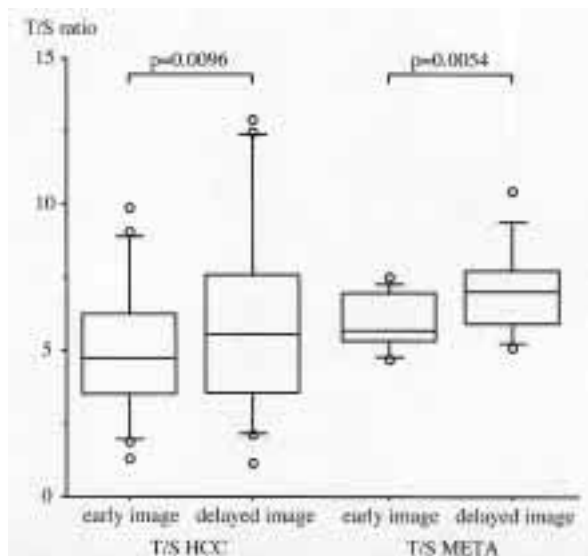


**Fig. 1** The T/S ratios of HCC and META in early and delayed images are shown. The T/S ratio of HCC in the delayed image is significantly higher than that in the early image, and the ratio of META in the delayed image is significantly higher than that in the early image.

*T/N ratio:*

In early images of HCCs, T/N ratios ranged from 1.01 to 4.00 (mean  $\pm$  SD =  $1.90 \pm 0.83$ ), whereas those in delayed images ranged from 1.16 to 6.11 (mean  $\pm$  SD =  $2.20 \pm 1.21$ ). In delayed images, T/N ratios increased in 11 of 18 HCC lesions, but there were no significant differences between early and delayed images in T/N ratios (Fig. 2).

In early images of META lesions, T/N ratios ranged from 1.45 to 2.92 (mean  $\pm$  SD =  $2.21 \pm 0.42$ ), whereas those in delayed images ranged from 2.37 to 4.89 (mean  $\pm$  SD =  $3.80 \pm 0.59$ ). In delayed images, T/N ratios had noticeably increased in all 15 lesions, and there were significant differences between early and delayed images ( $p = 0.0007$ ) (Fig. 2).

*N/S ratio:*

All 11 cases of HCC were complicated by LC, and N/S ratios in the early images ranged from 0.83 to 3.76 (mean  $\pm$  SD =  $2.58 \pm 0.99$ ), whereas those in delayed images

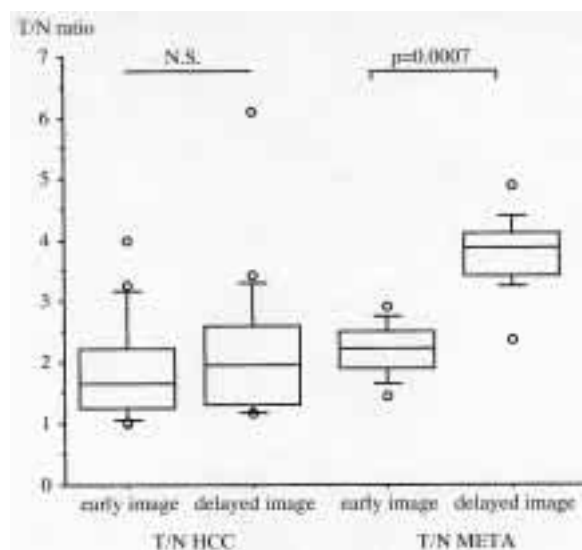


**Fig. 2** The T/N ratios of HCC and META in early and delayed images are shown. The T/N ratio of HCC in the delayed image is not significantly higher than that in the early image. The T/N ratio of META in the delayed image is markedly significant higher than that in the early image.

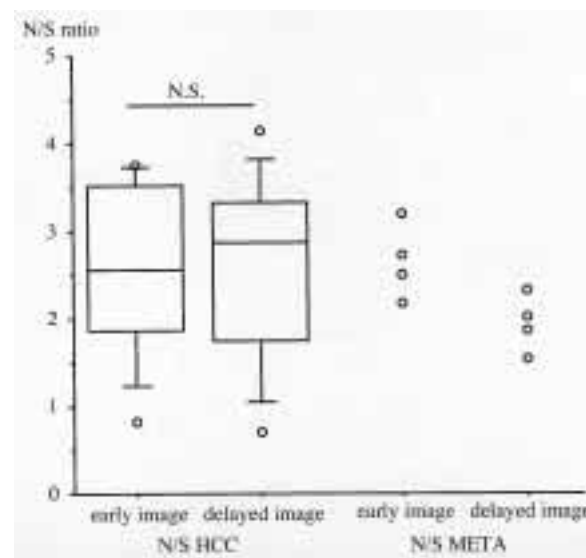
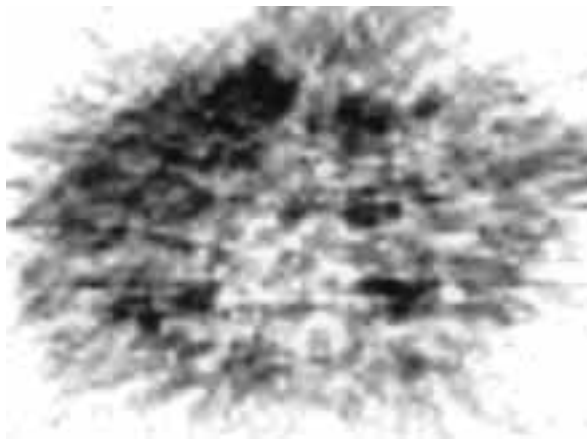


**Fig. 3** The N/S ratios of HCC and META in early and delayed images. There was no significant difference between the N/S ratio of HCC in the early and delayed images. The N/S ratios of META lesions were not statistically evaluated because the number of META cases was limited.

ranged from 0.71 to 4.14 (mean  $\pm$  SD =  $2.57 \pm 1.07$ ). In delayed images of HCCs, N/S ratios had increased in 4 cases, but had decreased in 7 cases. FDG accumulation between early and delayed images did not show a uniform tendency. In addition, there were no significant differences between early and delayed images of HCC cases in N/S ratios (Fig. 3).



A



C



B

**Fig. 4** The patient was a 65-year-old man with HCC recurring in S3 after right lobectomy. CT showed the early enhancement in the S3 liver margin, which showed low density during the late phase (A). Recurrent HCC was suspected on CT. Early images of FDG PET failed to depict FDG accumulation in the same region in visual judgment (B). Although the T/S ratio (4.20) was relatively high, the T/N ratio was as low as 1.14. While FDG accumulation was visually depicted by delayed images of FDG PET, and both T/S and T/N ratios were increased, 5.38 and 2.31, respectively (C). Therefore, delayed images of FDG PET facilitated the visual evaluation. Bilateral pelves were shown at the dorsal site (B, C).

All four cases of META were not complicated by LC or hepatitis. In early images of META cases, N/S ratios ranged from 2.13 to 3.24, whereas those in delayed images ranged from 1.57 to 2.34. No significance test could be done for N/S ratios of META cases due to the small number of samples, but all the N/S ratios had decreased in delayed images (Fig. 3).

#### Case presentation

The HCC case and the META case in which the usefulness of delayed images was confirmed are shown in Figures 4 and 5. Figure 4 shows a 65-year-old male with recurrent HCC in S3 after right lobectomy. The FDG accumulation in the HCC was not clearly seen in the early image, but intense FDG accumulation was seen in the delayed image. The CT and FDG PET of a 78-year-old male with multiple METAs in S4–S3 and S5 from colon carcinoma are shown in Figure 5. In this case, although FDG accumulation could be observed in early images, more intense FDG accumulation was shown in delayed images.

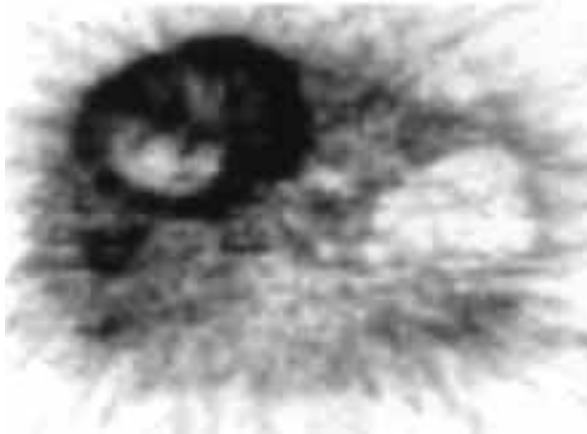
#### DISCUSSION

FDG PET has been recently reported as the method for evaluating various malignant tumors.<sup>1–5</sup> Since FDG is an analog of glucose, it is incorporated into the cell by glucose transporters as in glucose, and then converted to FDG-6 phosphate (FDG-6P) after phosphorylation by hexokinase.<sup>12</sup> FDG-6P is accumulated in the cell without receiving further conversion,<sup>12</sup> so that the level of regional glucose metabolism will be reflected by radioactivity in the tissue that includes the levels of FDG-6P accumulated in the cell and FDG incorporated into the cell by glucose transporters. FDG PET in liver tumors has been found to detect primary and metastatic lesions,<sup>6–10</sup> to differentiate benign tumors from malignant tumors,<sup>13</sup> and to evaluate therapeutic results,<sup>14–17</sup> but no difference between liver tumors and normal liver tissues in FDG accumulation has been reported in some liver tumors, especially in HCCs.

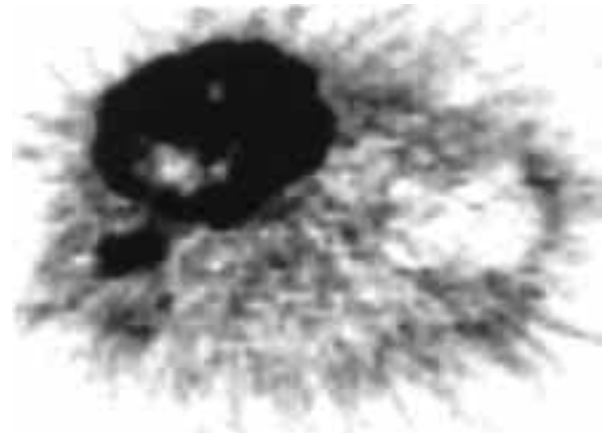
In most previous studies, FDG PET images were acquired about 1 hour after intravenous FDG administration, and we also acquired FDG PET images 45–55 minutes after FDG administration. Glucose metabolism is



A



B



C

**Fig. 5** The patient was a 78-year-old man with multiple META lesions in S4–S3 and S5 metastasized from colon carcinoma. CT revealed the presence of a large mass in S4–S3, in which a seemingly necrotic area without the enhancement was observed (A). In addition, a low-density area was also detected in S5. Although early images of FDG PET facilitated a visual evaluation of both lesions, levels of FDG accumulation were not high in either lesions (B). In these META lesions, T/S ratios were 5.65 and 5.29, respectively, while T/N ratios were 2.65 and 2.48, respectively. On the other hands, levels of FDG accumulation on delayed images were markedly higher than those on early images (C). Therefore, delayed images of FDG PET facilitated the visual evaluation of META lesions. On delayed images of FDG PET, the T/S ratios of both META lesions were 6.34 and 5.84, respectively, while T/N ratios were 4.05 and 3.73, respectively. Both T/S and T/N ratios on delayed images were higher than those on early images.

generally enhanced by increased hexokinase activity in tumors and FDG may gradually accumulate in tumor tissues,<sup>11</sup> so that tumors may be clearly visualized by FDG PET in contrast with normal tissues, because FDG accumulation in normal tissues may gradually decrease.<sup>11,12,18</sup>

Recently, the delayed image was reported to be useful for the detection of tumors and the differentiation between malignant and benign mass lesions.<sup>19,20</sup> By means of visual and quantitative analysis, this study evaluated whether visual improvement in delayed images compared with early images can be achieved in liver tumors when the time from FDG administration to image acquisition is prolonged.

As mentioned in our results, FDG accumulation in early and delayed images was detected in about half of the HCC lesions by visual analysis. Visual improvement was observed in only 6 HCC lesions. FDG accumulation in all META lesions was detected by visual analysis, and visual improvement was observed in all META cases. In addition, quantitative analysis showed significant differences between early and delayed images of META lesions both in T/N and T/S ratios. Nevertheless, only T/S ratios in

early images significantly differed from those in delayed images in HCC cases. In delayed images, increases in T/N and T/S ratios of META lesions were larger than those of HCCs.

In regard to the reasons for these findings, Gallagher et al. reported that levels of glucose-6-phosphatase (G-6 Pase), a dephosphorylation enzyme of FDG-6P, were exceptionally high in the liver and kidneys.<sup>21</sup> Okazumi et al. evaluated  $k_3$  levels, which reflect hexokinase activity, and  $k_4$  levels, which reflect G-6 Pase activity, by using a compartment model, and reported that  $k_4$  levels varied in HCC patients, although  $k_4$  levels were almost zero in patients with META lesions.<sup>6</sup> They noted that the  $k_3$  level was high and the  $k_4/k_3$  ratio was low in cirrhotic liver that showed signs of an FDG accumulation higher than that in normal liver. They also noted that the  $k_4/k_3$  ratio in hepatic tumor lesion was similar to that in normal liver when FDG accumulation in the hepatic tumor lesion was similar to that in the normal liver. Moreover, they reported that the  $k_4/k_3$  ratio in liver cancer was high when FDG accumulation in the hepatic tumor lesion was lower than that in the normal liver.<sup>6</sup>

Based on these findings, HCC lesions may exhibit various G-6 Pase activities. When the intracellular activity of G-6 Pase is high, FDG-6P accumulated in the cell is converted to FDG after dephosphorylation, thus returning to the blood stream. FDG cannot be accumulated in the cell, probably resulting in decreased FDG accumulation.<sup>22</sup> HCC lesions in this study were therefore thought to show various levels of FDG accumulation. Since META lesions seldom show signs of high G-6 Pase activity, FDG is serially incorporated and accumulated into the tumor as FDG-6P.

In this study, all HCC cases were complicated by LC. Almost no differences in C-P scores and clinical stages were seen among HCC cases, and there were neither significant differences nor a uniform trend in N/S ratios between early and delayed images of HCC cases. The presence or absence of significant differences in N/S ratios between both images was not evaluated in META cases, because of the small number of cases, but N/S ratios in delayed images were lower than those in early images in all META cases. This may be related to the fact that none of the patients with META lesions were complicated by LC or chronic hepatitis.

T/N ratios of HCCs were lower than those of META lesions in early and delayed images, probably because not only HCC lesions exhibit various G-6 Pase activities but also N/S ratios in HCC cases were not uniform due to complication by LC. That is, since the level of FDG accumulation in the non-tumor liver varied in HCC cases, there were no significant differences between early and delayed images in T/N ratios. Since N/S ratios in all META cases were decreased during the delayed phase, the degree of increase in T/N ratios on delayed images was noticeably larger than that in T/S ratios in delayed images.

Many small tumors should be false negative cases because partial volume effects result in lower FDG accumulations.<sup>23</sup> Hyperglycemia is also reported to reduce the FDG uptake in malignant pancreatic tumors, and detectability of malignant tumors decreases as a result.<sup>24</sup> In this study, the T/S ratio or T/N ratio and visual improvements did not show a uniform trend related to tumor size and BS level.

The level of diagnostic performance including sensitivity, specificity and accuracy of ultrasonography, CT and magnetic resonance imaging (MRI) for HCC is very high.<sup>25</sup> CT/MRI can detect small tumors, but these lesions frequently cannot be diagnosed as malignant or benign by these methods. FDG PET is functional metabolic imaging. In general, FDG PET is performed to assess malignant tumors, and the tumor activity is evaluated by the degree of FDG accumulation. Our results show that the acquisition of delayed FDG PET images can detect META lesions easily, so that delayed FDG PET images are clinically useful for assessing these lesions. Moreover, the acquisition of delayed FDG PET images may be very useful for evaluating chemotherapy therapeutic values for

META lesions, as well as for evaluating the number of META lesions or the level of tumor activity. Delayed images are expected to provide better diagnostic effects in FDG PET studies and to be used more frequently in diagnosing liver masses.

## CONCLUSION

In this study the usefulness of the FDG PET image obtained two hours after FDG injection was investigated and compared to that of images obtained after about one hour. The FDG PET imaging obtained after 2 hours had limited usefulness for hepatocellular carcinomas but was very useful for metastatic liver tumors. We therefore consider that FDG PET images should be obtained two hours after the injection to examine liver tumors.

## ACKNOWLEDGMENT

The authors are greatly indebted to the staff of the Department of Radiology of Osaka City University. The authors also thank PET chemistry staff and PET imaging technologists at Osaka City University for their contributions to this work.

## REFERENCES

1. Strauss LG, Conti PS. The applications of PET in clinical oncology. *J Nucl Med* 1991; 32: 623–648; discussion 649–650.
2. Choi JY, Kim SE, Shin HJ, Kim BT, Kim JH. Brain tumor imaging with <sup>99m</sup>Tc-tetrofosmin: comparison with <sup>201</sup>Tl, <sup>99m</sup>Tc-MIBI, and <sup>18</sup>F-fluorodeoxyglucose. *J Neurooncol* 2000; 46: 63–70.
3. Sazon DA, Santiago SM, Soo Hoo GW, Khonsary A, Brown C, Mandelkern M, et al. Fluorodeoxyglucose-positron emission tomography in the detection and staging of lung cancer. *Am J Respir Crit Care Med* 1996; 153: 417–421.
4. Keogan MT, Tyler D, Clark L, Branch MS, McDermott VG, DeLong DM, et al. Diagnosis of pancreatic carcinoma: role of FDG PET. *Am J Roentgenol* 1998; 171: 1565–1570.
5. Sugawara Y, Eisbruch A, Kosuda S, Recker BE, Kison PV, Wahl RL. Evaluation of FDG PET in patients with cervical cancer. *J Nucl Med* 1999; 40: 1125–1131.
6. Okazumi S, Isono K, Enomoto K, Kikuchi T, Ozaki M, Yamamoto H, et al. Evaluation of liver tumors using fluorine-18-fluorodeoxyglucose PET: characterization of tumor and assessment of effect of treatment [see comments]. *J Nucl Med* 1992; 33: 333–339.
7. Torizuka T, Tamaki N, Inokuma T, Magata Y, Sasayama S, Yonekura Y, et al. *In vivo* assessment of glucose metabolism in hepatocellular carcinoma with FDG-PET. *J Nucl Med* 1995; 36: 1811–1817.
8. Ogunbiyi OA, Flanagan FL, Dehdashti F, Siegel BA, Trask DD, Birnbaum EH, et al. Detection of recurrent and metastatic colorectal cancer: comparison of positron emission tomography and computed tomography [see comments]. *Ann Surg Oncol* 1997; 4: 613–620.
9. Messa C, Choi Y, Hoh CK, Jacobs EL, Glaspy JA, Pege S,

- et al. Quantification of glucose utilization in liver metastases: parametric imaging of FDG uptake with PET. *J Comput Assist Tomogr* 1992; 16: 684–689.
10. Lai DT, Fulham M, Stephen MS, Chu KM, Solomon M, Thompson JF, et al. The role of whole-body positron emission tomography with [<sup>18</sup>F]fluorodeoxyglucose in identifying operable colorectal cancer metastases to the liver. *Arch Surg* 1996; 131: 703–707.
  11. Di Chiro G. Positron emission tomography using [<sup>18</sup>F] fluorodeoxyglucose in brain tumors: a powerful diagnostic and prognostic tool. *Invest Radiol* 1987; 22: 360–371.
  12. Bida GT, Satyamurthy N, Barrio JR. The synthesis of 2-[<sup>18</sup>F]fluoro-2-deoxy-D-glucose using glycals: a reexamination. *J Nucl Med* 1984; 25: 1327–1334.
  13. Delbeke D, Martin WH, Sandler MP, Chapman WC, Wright JK Jr, Pinson CW. Evaluation of benign vs. malignant hepatic lesions with positron emission tomography. *Arch Surg* 1998; 133: 510–515; discussion 515–516.
  14. Torizuka T, Tamaki N, Inokuma T, Magata Y, Yonekura Y, Tanaka A, et al. Value of fluorine-18-FDG-PET to monitor hepatocellular carcinoma after interventional therapy. *J Nucl Med* 1994; 35: 1965–1969.
  15. Findlay M, Young H, Cunningham D, Iveson A, Cronin B, Hickish T, et al. Noninvasive monitoring of tumor metabolism using fluorodeoxyglucose and positron emission tomography in colorectal cancer liver metastases: correlation with tumor response to fluorouracil [see comments]. *J Clin Oncol* 1996; 14: 700–708.
  16. Enomoto K, Okazumi S, Fukunaga T, Asano T, Kikuchi T, Nagashima T, et al. The efficacy of <sup>18</sup>F-fluorodeoxyglucose positron emission tomography for the evaluation of hepatocellular carcinoma treatment (in Japanese). *Kanzo* 1993; 34: 464–470.
  17. Okazumi S, Enomoto K, Ozaki M, Yamamoto H, Yoshida M, Abe Y, et al. Evaluation of the effect of treatment for patients with liver tumors using <sup>18</sup>F-fluorodeoxyglucose PET (in Japanese). *KAKU IGAKU (Jpn J Nucl Med)* 1989; 26: 793–797.
  18. Knox WE, Jamdar SC, Davis PA. Hexokinase, differentiation and growth rates of transplanted rat tumors. *Cancer Res* 1970; 30: 2240–2244.
  19. Imdahl A, Nitzsche E, Krautmann F, Hogerle S, Boos S, Einert A, et al. Evaluation of positron emission tomography with 2-[<sup>18</sup>F]fluoro-2-deoxy-D-glucose for the differentiation of chronic pancreatitis and pancreatic cancer. *Br J Surg* 1999; 86: 194–199.
  20. Kubota K, Itoh M, Ozaki K, Ono S, Tashiro M, Yamaguchi K, et al. Advantage of delayed whole-body FDG-PET imaging for tumour detection. *Eur J Nucl Med* 2001; 28: 696–703.
  21. Gallagher BM, Fowler JS, Gutterson NI, MacGregor RR, Wan CN, Wolf AP. Metabolic trapping as a principle of radiopharmaceutical design: some factors responsible for the biodistribution of [<sup>18</sup>F] 2-deoxy-2-fluoro-D-glucose. *J Nucl Med* 19: 1154–1161, 1978.
  22. Fukuda H. Diagnosis of liver tumors with <sup>18</sup>F-FDG and <sup>18</sup>F-FDGal using PET (in Japanese). *Nippon Rinsho* 1991; 49: 1863–1867.
  23. Cremerius U, Fabry U, Neuerburg J, Zimny M, Osieka R, Buell U. Positron emission tomography with <sup>18</sup>F-FDG to detect residual disease after therapy for malignant lymphoma. *Nucl Med Commun* 1998; 19: 1055–1063.
  24. Zimny M, Bares R, Fass J, Adam G, Cremerius U, Dohmen B, et al. Fluorine-18 fluorodeoxyglucose positron emission tomography in the differential diagnosis of pancreatic carcinoma: a report of 106 cases. *Eur J Nucl Med* 1997; 24: 678–682.
  25. Peterson MS, Baron RL. Radiologic diagnosis of hepatocellular carcinoma. *Clin Liver Dis* 2001; 5: 123–144.